INTERNATIONAL JOURNAL OF
NUMERICAL ANALYSIS AND MODELING
Volume 12, Number 2, Pages 230–253

AN ADAPTIVE LINEAR TIME STEPPING ALGORITHM FOR SECOND-ORDER LINEAR EVOLUTION PROBLEMS

JUNJIANG LAI AND JIANGUO HUANG*

Abstract. In this paper, we propose and analyze a linear time stepping finite element method for abstract second order linear evolution problems. For such methods, we derive optimal order a posteriori error estimates and sharp a posteriori nodal error estimates using the energy approach and the duality argument. Based on these estimates, we further design an adaptive time stepping strategy for the previous discretization in time. Several numerical experiments are provided to show the reliability and efficiency of the a-posteriori error estimates and to assess the effectiveness of the proposed adaptive time stepping method.

Key words. A posteriori error analysis, adaptive algorithm, linear finite element, evolution problems.

1. Introduction

Adaptive time stepping methods are very important in developing efficient algorithms for solving evolution problems arising from fluid dynamics, epitaxial growth and many other applied sciences (cf. [15, 17, 22, 26, 27]). Such methods are able to adopt feasible time steps for time discretization, largely reducing the computational cost for getting numerical solutions with desired accuracy. The strategy for choosing time steps adaptively is very tricky and problem oriented, and one typical approach corresponds to the construction of an a-posteriori error estimator for the problem under discussion (cf. [6, 10]). Hence, a posteriori error analysis is very useful in constructing efficient adaptive time stepping methods.

In the past decade, people have witnessed rapid and sophisticated progresses in a posteriori error analysis for abstract first order evolution problems (cf. [1–4, 14]). One of the key points of the analysis in these references relies on a higher order reconstruction of the approximate solution, such that the reconstructed function is globally continuous as well as a quasi-projector of the approximate solution in some sense (cf. (3.4) in [3] and (2.7) in [4]). In light of this reconstructed function or its further modification, the optimal order a posteriori error analysis was established by the energy method. The a-posteriori superconvergence estimates for the error at the nodes for Galerkin and Runge-Kutta methods were also derived in [4].

However, to our knowledge, there are few results about a posteriori error analysis for abstract second order evolution problems (even in linear case), which frequently occur in structural analysis (cf. [9, 11, 12]). In the reference [5], Bernardi and Süli proposed a fully discrete scheme for the linear wave equation. The discretization for time derivatives is conducted by the backward Euler scheme with variable steps. In order to derive a posteriori error analysis, they first extended

Received by the editors February 27, 2014, and in revised form, November 10, 2014.
2000 *Mathematics Subject Classification.* 65M60, 65M15.
*Corresponding author.
The first author is supported by NSFC (Grant No. 11101199) and Program for New Century Excellent Talents in Fujian Province University (Grant No. JA12260). The second author is supported by NSFC (Grant No. 11171219) and E-Institutes of Shanghai Municipal Education Commission (Grant No. E03004).

the approximate solutions (the discrete displacement and velocity fields together) defined on time nodes to the whole time interval by linear interpolation, and then obtained a first-order system of error equations. Based on this system and a very technical derivation, they derived a posteriori error bound in time. Moreover, they also discussed a posterior error analysis in time and space together. In the reference [14], as an application of their a posteriori error analysis for abstract first-order problems, Makridakis and Nochetto obtained some a-posteriori error estimates for the second-order linear wave equation by reformatting it as a system of first-order equations; for details, see Corollaries 3.13 and 3.14 in [14]. In the reference [7], Georgoulis, Lakkis and Makridakis proposed a numerical method to solve a linear wave equation by discretizing the time derivatives via the central difference method and carrying out spatial discretization via the finite element method. They used a novel space-time reconstruction of the approximate solution (cf. Definition 4.1 in [7]) and some other techniques to achieve a posteriori $L^\infty(L^2)$-error bound for this method. Based on the time stepping method used in [11, 12], Huang, Lai and Tang proposed in [8] a discrete method for solving abstract second-order linear evolution problems and developed a posteriori error analysis systematically.

For the method in [8], we conduct the discretization of time derivatives by means of quadratic continuous discontinuous Galerkin (DG) method, so it has high accuracy in approximation. The computational overheads of the method involve numerical solution of a linear system with the linear operator having a 2 by 2 block structure. However, as is well-known, it is a challenging issue to develop fast solvers for such a system.

In order to balance the accuracy and computational cost, in this paper we propose and analyze linear time stepping methods for abstract second-order evolution problems. For this purpose, we first give the problem we are solving. For any real number $T > 0$, we want to find $u : [0, T] \to D(A)$ satisfying

$$\begin{cases} u''(t) + Au(t) = f(t), \quad 0 < t < T, \\ u(0) = u_0, \\ u'(0) = v_0, \end{cases} \tag{1}$$

where $(\cdot)'$ and $(\cdot)''$ denote respectively the first and second order derivatives in time, A is a positive definite, self-adjoint, linear operator on a Hilbert space $(H, \langle \cdot, \cdot \rangle)$ with domain $D(A)$ dense in H, and f is a function from $[0, T]$ into H. Throughout this paper, we assume that

$$u_0, v_0 \in D(A), \quad f \in L^2(0, T; H). \tag{2}$$

To simplify the presentation, we refer the reader to the monograph [25] for details about the standard notation corresponding to the above problem.

To discretize problem (1), we use a standard finite element approach for handling second-order evolution problems, see, e.g., [11–13]. We first define a non-uniform subdivision for the time interval $I := (0, T)$:

$$0 = t_0 < t_1 < \cdots < t_N = T,$$

and use the notations

$$J_n = (t_{n-1}, t_n], \quad k_n = t_n - t_{n-1}, \quad 1 \le n \le N.$$

Define

$$\mathcal{V}_1 = \left\{ v : \bar{I} \to D(A); v \in C(\bar{I}),\ v|_{J_n}(t) = \sum_{j=0}^{1} t^j w_j,\ w_j \in D(A),\ 1 \le n \le N \right\},$$

$$\mathcal{W}_2 = \left\{ v : \bar{I} \to D(A); v \in C^1(\bar{I}),\ v|_{J_n}(t) = \sum_{j=0}^{2} t^j w_j,\ w_j \in D(A),\ 1 \le n \le N \right\},$$

$$\mathcal{H}_q = \left\{ v : \bar{I} \to H; v|_{J_n}(t) = \sum_{j=0}^{q} t^j w_j,\ w_j \in H,\ 1 \le n \le N \right\},\quad q = 0,\ 1.$$

Let $\mathcal{V}_1(J_n)$ and $\mathcal{W}_2(J_n)$ consist of the restrictions to J_n of the elements of $\mathcal{V}_1$ and $\mathcal{W}_2$, respectively. Similarly, denote by $\mathcal{H}_q(J_n)$ the restriction of $\mathcal{H}_q$ to J_n. Then our linear time stepping finite element method for (1) is to find $U \in \mathcal{V}_1$ such that

$$\text{(3)} \qquad \begin{cases} \displaystyle\int_{J_n} \big(\langle U'',\, w'\rangle + \langle F(t,\, U),\, w'\rangle\big)\,\mathrm{d}t + \langle \dot{U}_+^{n-1} - \dot{U}_-^{n-1},\, \dot{w}_+^{n-1}\rangle = 0 \\ \qquad\qquad\qquad\qquad\qquad\qquad \forall\, w \in \mathcal{V}_1(J_n), \quad 1 \le n \le N, \\ U^0 = u_0, \quad \dot{U}_-^0 = v_0, \end{cases}$$

where

$$\dot{w}_\pm^{n-1} := \lim_{s \to 0^+} w'(t_{n-1} \pm s), \quad w^{n-1} := w(t_{n-1}), \quad F(t,\, U) := AU - f(t).$$

The method (3) is a continuous discontinuous Galerkin (DG) method. For completeness, we simply show how to derive it based on the DG method for the first-order evolution equation. Letting $v = u'$, the equation in (1) can be rewritten as $v' + F(t, u) = 0$. Let $U \in \mathcal{V}_1$ be the approximate solution of u; let V be the approximate solution of v, which is assumed to lie in $\mathcal{V}_1' := \{w';\ w \in \mathcal{V}_1\}$. Then according to the DG method for the first-order evolution equation (see, e.g., (2.3) in [4] or (12.4) in [23]), we know V is determined by

$$\int_{J_n} \big(\langle V',\, w'\rangle + \langle F(t,\, U),\, w'\rangle\big)\,\mathrm{d}t + \langle V(t_{n-1}+0) - V(t_{n-1}-0),\, \dot{w}_+^{n-1}\rangle = 0 \quad \forall\, w \in \mathcal{V}_1(J_n).$$

Now, unlike the usual way to set up a variational equation between V and U to enforce the relation $v = u'$, we directly require that $V = U'$ and thus obtain (3) from the above equation.

We know $U \in \mathcal{V}_1$ is continuous at $t = t_n$ and its restriction to any J_n is a first order polynomial in the variable t, so $U|_{J_n}$ is uniquely determined by $\dot{U}_-^n$ and U^{n-1}, i.e.,

$$\text{(4)} \qquad U(t) = U^{n-1} + (t - t_{n-1})\dot{U}_-^n, \quad t \in J_n.$$

Inserting (4) into the first equation of (3) and on J_n taking w' to be any element φ in $D(A)$, we have by some direct manipulation that an explicit formulation of this method is to find $\{\dot{U}_-^n\}_{n=1}^N$ such that

$$\text{(5)} \qquad \begin{aligned} &\frac{k_n^2}{2}\langle A\dot{U}_-^n,\, \varphi\rangle + \langle \dot{U}_-^n,\, \varphi\rangle \\ &= -k_n\langle AU^{n-1},\, \varphi\rangle + \langle \dot{U}_-^{n-1},\, \varphi\rangle + \int_{J_n} \langle f,\, \varphi\rangle\,\mathrm{d}t \quad \forall\, \varphi \in D(A), 1 \le n \le N. \end{aligned}$$

Now let us discuss the implementation of the scheme (5). In fact, if the function U is obtained on J_{n-1}, then $\dot{U}_-^{n-1}$ and U^{n-1} are available. Thus, we can obtain

$\dot{U}_-^n$ by solving the linear system (5), and hence the function U on J_n is available too. In this way, we can obtain the function U in the whole time interval $\bar{I}$. In other words, at each time step, we have only to solve a linear system with the linear operator having 1-by-1 block structure, which can be solved very conveniently.

In order to develop reliable a posteriori error analysis for our method (3), we require to technically devise a higher order reconstruction $\tilde{U}$ from U in advance. Motivated by the ideas in higher order reconstruction for numerical solutions of first-order evolution problems (cf. [1–4, 14]), we successfully work out the answer. Our key observation is that, not like the first-order evolution problem, the reconstructed function for the second-order evolution problem must be C^1-smooth as well as a quasi-projector of the approximate solution U. To be more precise, $\widetilde{U}$ is uniquely determined by the relations (7)-(8), which satisfies the variational equation (9). Using this reconstruction and the energy method, we can derive optimal a posteriori error estimates for $(u-U)'$. Moreover, we can also derive sharp a posteriori error estimator at the time nodes, by means of the duality method as given in [11, 12]. Similar to [8], based on the available a posteriori error estimates, using the error equidistribution strategy (cf. [6, 16]), and following some ideas implied in the Runge-Kutta-Felberg method (cf. [21]), we are able to devise an adaptive time stepping method related to (3). We perform several numerical examples to show the reliability and efficiency of our a posteriori error estimates (estimators) as well as the effectiveness of the adaptive time stepping method proposed.

The remainder of this paper is organized as follows. The higher order reconstruction $\tilde{U}$ from U and the corresponding optimal a posteriori error analysis are given in Section 2. The sharp a posteriori error estimator at the time nodes is obtained in Section 3. The adaptive time stepping method is devised and discussed in Section 4. In Section 5, several numerical experiments are performed to illustrate the reliability and efficiency of our a posteriori error estimates (estimators) and to assess the effectiveness of our adaptive time stepping method.

2. Optimal a posteriori error analysis

Let $e := u - U$, with U given by (3). The usual way for bounding the error e is to use the corresponding error equation $e''(t) + Ae(t) = -R(t)$, where the residual $R(t)$ is defined by

$$R(t) = U''(t) + AU(t) - f(t), \quad t \in J_n, \tag{6}$$

or equivalently,

$$R = -(u-U)'' - A(u-U)$$

in view of (1). However, by the error analysis for finite elements, the magnitude of the quantity $R(t)$ is $O(1)$, and hence we can not derive sharp estimate for the error $e(t)$ through the previous error equation. As an instance, consider an ordinary differential equation $u''(t) = f(t) = d$ with $d \neq 0$ a real constant. From (4) and (6), we have

$$R(t) = -f(t) = -d, \quad t \in J_n,$$

so $R(t)$ is indeed of the size $O(1)$ in this case.

Therefore, as in [1–4, 8, 14], we require a higher order reconstruction $\tilde{U}$ from U, to establish optimal a posteriori error analysis.

2.1. Reconstruction. We first introduce an invertible linear operator $\widetilde{I}_2$: $\mathcal{V}_1 \to \mathcal{W}_2$ as follows. With every $w \in \mathcal{V}_1$ we associate an element $\widetilde{w} := \widetilde{I}_2 w \in \mathcal{W}_2$ satisfied

by

$$\begin{cases} \widetilde{w}(t_0) = w(t_0), \\ \widetilde{w}'(t_0) = v_0, \\ \widetilde{w}'(t_1) = \dot{w}_-^1 \end{cases} \tag{7}$$

on the first subinterval J_1 and

$$\begin{cases} \widetilde{w}'(t_{n-1}) = \dot{w}_-^{n-1}, \\ \widetilde{w}'(t_n) = \dot{w}_-^n \end{cases} \tag{8}$$

on other subinterval $J_n (2 \le n \le N)$. We call $\widetilde{w}$ a time reconstruction of w. Conversely, if $\widetilde{w} \in \mathcal{W}_2$ is given and $I_1 : \mathcal{W}_2 \to \mathcal{V}_1$ is the interpolation operator satisfied by

$$\begin{cases} (I_1\varphi)(t_0) = \varphi(t_0), \\ (\dot{I_1\varphi})_-^1 = \varphi'(t_1) \end{cases}$$

on the first subinterval J_1 and

$$(\dot{I_1\varphi})_-^n = \varphi'(t_n)$$

on other subinterval $J_n (2 \le n \le N)$. We can recover w locally via interpolation, i.e., $w = I_1\widetilde{w}$. Thus, $I_1 = \widetilde{I}_2^{-1}$.

Using the reconstruction $\widetilde{U} \in \mathcal{W}_2$ of $U \in \mathcal{V}_1$ which is the solution of (3), we can deduce from (7)-(8) that for $w \in \mathcal{V}_1(J_n)$,

$$\begin{aligned} \int_{J_n} \langle \widetilde{U}'', w' \rangle \, \mathrm{d}t &= \langle \widetilde{U}'(t_n), \dot{w}_+^{n-1} \rangle - \langle \widetilde{U}'(t_{n-1}), \dot{w}_+^{n-1} \rangle \\ &= \langle \dot{U}_+^{n-1} - \dot{U}_-^{n-1}, \dot{w}_+^{n-1} \rangle \\ &= \langle \dot{U}_+^{n-1} - \dot{U}_-^{n-1}, \dot{w}_+^{n-1} \rangle + \int_{J_n} \langle U'', w' \rangle \, \mathrm{d}t. \end{aligned} \tag{9}$$

Inserting (9) into (3) readily gives

$$\int_{J_n} \big(\langle \widetilde{U}'', w' \rangle + \langle F(t, I_1\widetilde{U}), w' \rangle \big) \, \mathrm{d}t = 0 \quad \forall\, w \in \mathcal{V}_1(J_n), \quad 1 \le n \le N,$$

i.e.,

$$\widetilde{U}'' + P_0 F(t, I_1\widetilde{U}) = 0 \quad \forall\, t \in J_n, \tag{10}$$

where $P_q \, (q = 0, 1)$ is the (local) L^2 orthogonal projection operator onto $\mathcal{H}_q(J_n)$ (cf. [4]). Consequently, for each n,

$$\int_{J_n} \langle P_q v - v, w \rangle \, \mathrm{d}t = 0 \quad \forall\, w \in \mathcal{H}_q(J_n).$$

Recall that $\widetilde{U}$ is C^1-continuous on $\bar{I}$ and its restriction to any J_n is a second order polynomial in the variable t, so $\widetilde{U}|_{J_n}$ is uniquely determined by $\widetilde{U}^{n-1}$, $\dot{U}_-^{n-1}$ and $\dot{U}_-^n$. If we get the function $\widetilde{U}$ on J_{n-1}, then $\widetilde{U}^{n-1}$ is available. Hence, the function $\widetilde{U}$ on J_n is available too. In this way, we can obtain the function $\widetilde{U}$ in the whole time interval $\bar{I}$. In fact, we have by some direct manipulation that (cf. [18, 20]), for $t \in J_n$, $1 \le n \le N$,

$$\widetilde{U}(t) = \widetilde{U}^{n-1} + k_n \dot{U}_-^{n-1} \phi_0 \left(\frac{t - t_{n-1}}{k_n} \right) + k_n \dot{U}_-^n \phi_1 \left(\frac{t - t_{n-1}}{k_n} \right),$$

where

$$\phi_0(\xi) = -\frac{1}{2}\xi^2 + \xi, \quad \phi_1(\xi) = \frac{1}{2}\xi^2.$$

Therefore,

$$\widetilde{U}''(t) = \frac{1}{k_n}(\dot{U}_-^n - \dot{U}_-^{n-1}), \quad t \in J_n. \tag{11}$$

On the other hand, observing that

$$U(t) = U^{n-1} + k_n \dot{U}_+^{n-1}\phi_0\left(\frac{t-t_{n-1}}{k_n}\right) + k_n \dot{U}_-^n \phi_1\left(\frac{t-t_{n-1}}{k_n}\right),$$

we know

$$\begin{aligned} U(t) - \widetilde{U}(t) &= k_n(\dot{U}_+^{n-1} - \dot{U}_-^{n-1})\phi_0\left(\frac{t-t_{n-1}}{k_n}\right) + U^{n-1} - \widetilde{U}^{n-1} \\ &= k_n^2 \widetilde{U}''(t)\phi_0\left(\frac{t-t_{n-1}}{k_n}\right) + U^{n-1} - \widetilde{U}^{n-1}, \quad t \in J_n. \end{aligned} \tag{12}$$

Hence,

$$U^n - \widetilde{U}^n = \frac{1}{2}k_n^2 \widetilde{U}''(t) + U^{n-1} - \widetilde{U}^{n-1}, \quad t \in J_n,$$

which implies

$$U^n - \widetilde{U}^n = \frac{1}{2}\sum_{m=1}^{n} k_m^2 \widetilde{U}''|_{J_m}. \tag{13}$$

2.2. Energy estimates. Let $V := D(A^{1/2})$ and denote the norms in H and in V by $|\cdot|$ and $\|\cdot\|$, with $\|v\| := |A^{1/2}v| = \langle Av, v\rangle^{1/2}$, respectively. We also use the following norm notations:

$$\|v\|_{L^\infty(G)} := \operatorname*{ess\,sup}_{t\in G} \|v(t)\|, \quad |v|_{L^\infty(G)} := \operatorname*{ess\,sup}_{t\in G} |v(t)|.$$

Under the assumption (2), we know from [19, 25] that there exists a unique weak solution $u \in C([0, T]; V)\bigcap C^1([0, T]; H)$ to the evolution problem (1).

Let $\widetilde{R}$ be the residual of $\widetilde{U}$ given by

$$\widetilde{R}(t) := \widetilde{U}''(t) + A\widetilde{U} - f(t), \quad t \in J_n,\ 1 \le n \le N. \tag{14}$$

Subtracting (14) from the differential equation in (1), we readily have

$$\widetilde{e}''(t) + A\widetilde{e} = -\widetilde{R}(t), \tag{15}$$

where $\widetilde{e} := u - \widetilde{U}$. Testing (15) with $\widetilde{e}'$ and integrating over $t \in [0, \tau]$ gives

$$\int_0^\tau \big(\langle \widetilde{e}''(s), \widetilde{e}'(s)\rangle + \langle A\widetilde{e}(s), \widetilde{e}'(s)\rangle\big)\,\mathrm{d}s = \int_0^\tau \langle -\widetilde{R}(s), \widetilde{e}'(s)\rangle\,\mathrm{d}s.$$

Using the fact that $\widetilde{e}(0) = \widetilde{e}'(0) = 0$ and integration by parts gives

$$\frac{1}{2}|\widetilde{e}'(\tau)|^2 + \frac{1}{2}\|\widetilde{e}(\tau)\|^2 = \int_0^\tau \langle -\widetilde{R}(s), \widetilde{e}'(s)\rangle\,\mathrm{d}s, \quad \tau \in [0, t], \tag{16}$$

and hence

$$\begin{aligned} &\frac{1}{2}\big(\max_{0\le\tau\le t}|\widetilde{e}'(\tau)|\big)^2 \\ \le\ &\max_{0\le\tau\le t}\int_0^\tau |\langle \widetilde{R}(s), \widetilde{e}'(s)\rangle|\,\mathrm{d}s \\ \le\ &\int_0^t |\langle \widetilde{R}(s), \widetilde{e}'(s)\rangle|\,\mathrm{d}s \le \max_{0\le\tau\le t}|\widetilde{e}'(\tau)|\int_0^t |\widetilde{R}(s)|\,\mathrm{d}s. \end{aligned}$$

In other words,

$$\max_{0\le\tau\le t}|\widetilde{e}'(\tau)| \le 2\int_0^t |\widetilde{R}(s)|\,\mathrm{d}s. \tag{17}$$

Now, it follows from (16)-(17) that

$$\begin{aligned}\frac{1}{2}\big(\max_{0\le\tau\le t}\|\widetilde{e}(\tau)\|\big)^2 &\le \int_0^t |\langle \widetilde{R}(s),\, \widetilde{e}'(s)\rangle|\,\mathrm{d}s\\ \le \max_{0\le\tau\le t}|\widetilde{e}'(\tau)|\int_0^t |\widetilde{R}(s)|\,\mathrm{d}s &\le 2\big(\int_0^t |\widetilde{R}(s)|\,\mathrm{d}s\big)^2,\end{aligned}$$

i.e.,

$$\max_{0\le\tau\le t}\|\widetilde{e}(\tau)\| \le 2\int_0^t |\widetilde{R}(s)|\,\mathrm{d}s.$$

It is evident by the triangle inequality that

$$|(U-\widetilde{U})'|_{L^\infty(0,\,t)} \le |(u-U)'|_{L^\infty(0,\,t)} + \max_{0\le\tau\le t}|(u-\widetilde{U})'(\tau)|.$$

Summarizing the above results, we can get a posteriori error estimates for the method (3), as described in the following theorem.

Theorem 2.1. *Let u and U be the solutions of* (1) *and* (3)*, respectively, and let $\widetilde{U}$ be the reconstruction of U by* (7)-(8)*. Then, for $t\in[0,\,T]$, there hold the following a posteriori error estimates:*

$$\begin{aligned}\max_{0\le\tau\le t}\big|(u-\widetilde{U})'(\tau)\big| &\le 2\int_0^t |\widetilde{R}(s)|\,\mathrm{d}s,\\ \max_{0\le\tau\le t}\big\|(u-\widetilde{U})(\tau)\big\| &\le 2\int_0^t |\widetilde{R}(s)|\,\mathrm{d}s,\end{aligned} \tag{18}$$

where the a-posteriori quantity $\widetilde{R}$ is given by (14)*. Moreover, we have the following lower estimate:*

$$|(U-\widetilde{U})'|_{L^\infty(0,\,t)} \le |(u-U)'|_{L^\infty(0,\,t)} + \max_{0\le\tau\le t}|(u-\widetilde{U})'(\tau)|.$$

Let $l_1(t) := \sqrt{\frac{3}{2}}t$ be the second orthonormal Legendre polynomial in $[-1,\,1]$. And write

$$t_{n,*} := \frac{t_{n-1}+t_n}{2},\quad 1\le n\le N.$$

Lemma 2.2. *For $s\in J_n$, $1\le n\le N$,*

$$U(s) - P_0U(s) = (s-t_{n,*})U'(s).$$

Moreover, for $t\in J_n$, $1\le n\le N$, there holds

$$\begin{aligned}2\int_0^t |\widetilde{R}(s)|\,\mathrm{d}s \le \sum_{m=1}^{n}\Big(&\frac{2}{3}k_m^3|A\widetilde{U}''|_{L^\infty(J_m)} + k_m^2 t|A\widetilde{U}''|_{L^\infty(J_m)}\\ &+\frac{1}{2}k_m^2|AU'|_{L^\infty(J_m)} + 2\int_{J_m}|f(s)-P_0f(s)|\,\mathrm{d}s\Big).\end{aligned} \tag{19}$$

Proof. Let p_1 be the second Legendre polynomial shifted to J_n and normalized, i.e.,

$$p_1(t) = \sqrt{\frac{2}{k_n}}l_1\left(\frac{2t-t_{n-1}-t_n}{k_n}\right),\quad t\in J_n.$$

Noting that

$$U(s) - P_0U(s) = P_1U(s) - P_0U(s) = \int_{J_n} U(t)p_1(t)\,\mathrm{d}t \cdot p_1(s),$$

we have

$$(U - P_0U)(t_{n,*}) = 0,$$

from which it follows that

$$U(s) - P_0U(s) = (s - t_{n,*})U'(s), \quad s \in J_n. \tag{20}$$

From (10) and (14), $\widetilde{R}(s)$ can be expressed as

$$\widetilde{R}(s) = A(\widetilde{U} - U)(s) + A(U - P_0U)(s) - (f - P_0f)(s). \tag{21}$$

Using (12)-(13) and (20)-(21), we can obtain (19) by some direct manipulation. □

We then differentiate (12) with respect to t to get

$$(U - \widetilde{U})'(t) = (t_n - t)\widetilde{U}''(t), \quad t \in J_n,$$

leading to

$$|(U - \widetilde{U})'|_{L^\infty(J_n)} = k_n|\widetilde{U}''|_{L^\infty(J_n)}, \quad 1 \le n \le N. \tag{22}$$

Applying (18), (22) and noting that

$$|(u - U)'|_{L^\infty(0,\,t)} \le \max_{0\le\tau\le t} \big|(u - \widetilde{U})'(\tau)\big| + |(U - \widetilde{U})'|_{L^\infty(0,\,t)},$$

we obtain the following result.

Theorem 2.3. *Let u and U be the solutions of* (1) *and* (3)*, respectively, and let $\widetilde{U}$ be the reconstruction of U by* (7)-(8)*. Then, for $t \in J_n$, $1 \le n \le N$, there holds*

$$|(u - U)'|_{L^\infty(0,\,t)} \le \max_{1\le m\le n} k_m|\widetilde{U}''|_{L^\infty(J_m)} + 2\int_0^t |\widetilde{R}(s)|\,\mathrm{d}s. \tag{23}$$

The following result is a direct consequence of Theorems 2.1, 2.3 and (22).

Corollary 2.4. *Let u and U be the solutions of* (1) *and* (3)*, respectively, and let $\widetilde{U}$ be the reconstruction of U by* (7)-(8)*. Then, for $t \in J_n$, $1 \le n \le N$, there hold the following lower and upper bounds:*

$$\begin{aligned}
&\max_{1\le m\le n} k_m|\widetilde{U}''|_{L^\infty(J_m)} \\
&\le |(u - U)'|_{L^\infty(0,\,t)} + \max_{0\le\tau\le t} \big|(u - \widetilde{U})'(\tau)\big| \\
&\le \max_{1\le m\le n} k_m|\widetilde{U}''|_{L^\infty(J_m)} + 4\int_0^t |\widetilde{R}(s)|\,\mathrm{d}s,
\end{aligned}$$

where the a-posteriori quantity $\widetilde{R}$ is given by (14)*.*

From (11), the a-posteriori error estimate given in Theorem 2.3 can be expressed as

$$|(u - U)'|_{L^\infty(0,\,t)} \le \max_{1\le m\le n} |\dot{U}_+^{m-1} - \dot{U}_-^{m-1}| + 2\int_0^t |\widetilde{R}(s)|\,\mathrm{d}s,$$

which is quite similar to the a-posteriori error estimate corresponding to the finite element method in space (cf. [24]).

In what follows, we shall establish several stability estimates for the linear time stepping finite element method. To simplify the presentation, write

$$\bar{f}^m := k_m^{-1}\int_{J_m} f(t)\,\mathrm{d}t, \quad [\![\dot{U}]\!]_{m-1} := \dot{U}_-^m - \dot{U}_-^{m-1}, \quad 1 \le m \le N.$$

First of all, it follows from (10) that

$$\widetilde{U}''|_{J_m} + \frac{1}{2}A(U^m + U^{m-1}) = \bar{f}^m, \quad 1 \le m \le N. \tag{24}$$

Theorem 2.5. *Let U be the solution of (3), and let $\widetilde{U}$ be the reconstruction of U by (7)-(8). If $u_0 \in D(A^2)$, $v_0 \in D(A^{3/2})$ and $f \in L^2(0,T;D(A^{3/2}))$, then the following stability estimates hold for $1 \le m \le N$:*

$$|U'|_{L^\infty(J_m)} \le C\Big(|A^{1/2}u_0|^2 + |v_0|^2 + \sum_{l=1}^{m} k_l|\bar{f}^l|^2\Big)^{1/2},$$

$$|\widetilde{U}''|_{L^\infty(J_m)} \le C\Big(|Au_0|^2 + |A^{1/2}v_0|^2 + |\bar{f}^m|^2 + \sum_{l=1}^{m} k_l|A^{1/2}\bar{f}^l|^2 + \sum_{l=1}^{m}\sum_{p=1}^{l} k_l k_p|A^{1/2}\bar{f}^p|^2\Big)^{1/2},$$

$$|AU'|_{L^\infty(J_m)} \le C\Big(|A^{3/2}u_0|^2 + |Av_0|^2 + \sum_{l=1}^{m} k_l|A\bar{f}^l|^2\Big)^{1/2}, \tag{25}$$

$$|A\widetilde{U}''|_{L^\infty(J_m)} \le C\Big(|A^2u_0|^2 + |A^{3/2}v_0|^2 + |A\bar{f}^m|^2 + \sum_{l=1}^{m} k_l|A^{3/2}\bar{f}^l|^2 + \sum_{l=1}^{m}\sum_{p=1}^{l} k_l k_p|A^{3/2}\bar{f}^p|^2\Big)^{1/2}, \tag{26}$$

where C is a positive constant independent of the time step size, which may take different values in different appearances.

Proof. Testing the scheme (24) with $2k_m\dot{U}_-^m$ and using (11), we have

$$2\langle \dot{U}_-^m - \dot{U}_-^{m-1}, \dot{U}_-^m\rangle + \langle AU^m, U^m\rangle - \langle AU^{m-1}, U^{m-1}\rangle = 2k_m\langle \bar{f}^m, \dot{U}_-^m\rangle. \tag{27}$$

Summing this equation with respect to m implies

$$\begin{aligned}\langle \dot{U}_-^m, \dot{U}_-^m\rangle + \sum_{l=0}^{m-1}\langle [\![\dot{U}]\!]_l, [\![\dot{U}]\!]_l\rangle + \langle AU^m, U^m\rangle &= \langle Au_0, u_0\rangle + \langle v_0, v_0\rangle + \sum_{l=1}^{m} 2k_l\langle \bar{f}^l, \dot{U}_-^l\rangle \\ &\le \langle Au_0, u_0\rangle + \langle v_0, v_0\rangle + \sum_{l=1}^{m} 2k_l\big|\langle \bar{f}^l, \dot{U}_-^l\rangle\big|, \end{aligned} \tag{28}$$

from which we get

$$\langle \dot{U}_-^m, \dot{U}_-^m\rangle \le \langle Au_0, u_0\rangle + \langle v_0, v_0\rangle + \sum_{l=1}^{m} 2k_l\langle \bar{f}^l, \bar{f}^l\rangle^{1/2}\langle \dot{U}_-^l, \dot{U}_-^l\rangle^{1/2}.$$

Applying the discrete Gronwall lemma (cf. [18]) to the above inequality, we further have

$$|U'|_{L^\infty(J_m)} = |\dot{U}_-^m| \le C\Big(|A^{1/2}u_0|^2 + |v_0|^2 + \sum_{l=1}^{m} k_l|\bar{f}^l|^2\Big)^{1/2}. \tag{29}$$

Next, we apply A to the scheme (24) to get

$$A\widetilde{U}''|_{J_m} + \frac{1}{2}A^2(U^m + U^{m-1}) = A\bar{f}^m, \quad 1 \le m \le N,$$

and using the similar argument for deriving (27)-(28) we know

$$\begin{aligned}\langle A^{1/2}\dot{U}_-^m,\, A^{1/2}\dot{U}_-^m\rangle &+ \sum_{l=0}^{m-1}\big\langle A[\![\dot{U}]\!]_l,\, [\![\dot{U}]\!]_l\big\rangle + \langle AU^m,\, AU^m\rangle \\ &= \langle Au_0,\, Au_0\rangle + \langle Av_0,\, v_0\rangle + \sum_{l=1}^{m} 2k_l\langle A^{1/2}\bar{f}^l,\, A^{1/2}\dot{U}_-^l\rangle \\ &\le \langle Au_0,\, Au_0\rangle + \langle Av_0,\, v_0\rangle + \sum_{l=1}^{m} 2k_l\big|\langle A^{1/2}\bar{f}^l,\, A^{1/2}\dot{U}_-^l\rangle\big|,\end{aligned}$$

from which we deduce

$$\langle A^{1/2}\dot{U}_-^m,\, A^{1/2}\dot{U}_-^m\rangle \le C\Big(\langle Au_0,\, Au_0\rangle + \langle Av_0,\, v_0\rangle + \sum_{l=1}^{m} k_l\langle A^{1/2}\bar{f}^l,\, A^{1/2}\bar{f}^l\rangle\Big),$$

and hence

$$\begin{aligned}\langle AU^m,\, AU^m\rangle \le C\Big(&\langle Au_0,\, Au_0\rangle + \langle Av_0,\, v_0\rangle + \sum_{l=1}^{m} k_l\langle A^{1/2}\bar{f}^l,\, A^{1/2}\bar{f}^l\rangle \\ &+ \sum_{l=1}^{m}\sum_{p=1}^{l} k_lk_p\langle A^{1/2}\bar{f}^p,\, A^{1/2}\bar{f}^p\rangle\Big).\end{aligned}$$

This combined with the scheme (24) and the triangle inequality gives

$$\begin{aligned}|\widetilde{U}''|_{L^\infty(J_m)} = \big|\widetilde{U}''|_{J_m}\big| \le{}& |\bar{f}^m| + \frac{1}{2}|AU^m| + \frac{1}{2}|AU^{m-1}| \\ \le{}& C\Big(|Au_0|^2 + |A^{1/2}v_0|^2 + |\bar{f}^m|^2 \\ &+ \sum_{l=1}^{m} k_l|A^{1/2}\bar{f}^l|^2 + \sum_{l=1}^{m}\sum_{p=1}^{l} k_lk_p|A^{1/2}\bar{f}^p|^2\Big)^{1/2}.\end{aligned} \tag{30}$$

Applying A^2 and A^3 to the scheme (24) and arguing as in the derivation of (29) and (30), we can obtain (25)-(26) accordingly. □

Remark 2.6. Suppose that $u_0 \in D(A^2)$, $v_0 \in D(A^{3/2})$, and f lies in $L^2(0,T;D(A^{3/2}))$ and admits one time derivative. Then we can check from (19) and Theorem 2.5 that the magnitude of the quantity $\int_0^t |\widetilde{R}(s)|\,\mathrm{d}s$ is of order 1 with respect to the time step k_m. Hence, noting that U is a piecewise polynomial of degree 1, we get the optimal order (1 order) a posteriori error estimates for the time derivative of the error $u - U$ (cf. Theorem 2.3 and Corollary 2.4).

3. Nodal error estimates

In this section, we intend to apply the duality method (cf. [11, 12]) to derive a posteriori error estimates at the time nodes.

For $n \in \{1, \ldots, N\}$, let g be the solution of the following backward homogeneous problem

$$\begin{cases} g''(t) + Ag(t) = 0, \quad 0 < t < t_n, \\ g(t_n) = \mu, \\ g'(t_n) = \nu. \end{cases} \tag{31}$$

It is straightforward that

$$\int_t^{t_n} \langle g'' + Ag,\, g' \rangle \,\mathrm{d}t = 0,$$

which together with the integration by parts implies

$$\|g(t)\|^2 + |g'(t)|^2 = \|\mu\|^2 + |\nu|^2, \quad t \in [0,\, t_n]. \tag{32}$$

Now, choosing $\mu = 0$, $\nu = \widetilde{e}'(t_n)$ in (31) we arrive at

$$\begin{aligned}
|\dot{e}_-^n|^2 = |\widetilde{e}'(t_n)|^2 &= \int_0^{t_n} \langle \widetilde{e}',\, g' \rangle' \,\mathrm{d}t = \int_0^{t_n} \big(\langle \widetilde{e}'',\, g' \rangle + \langle \widetilde{e}',\, g'' \rangle \big) \,\mathrm{d}t \\
&= \int_0^{t_n} \big(\langle \widetilde{e}'',\, g' \rangle - \langle \widetilde{e}',\, Ag \rangle \big) \,\mathrm{d}t = \int_0^{t_n} \big(\langle \widetilde{e}'',\, g' \rangle + \langle \widetilde{e},\, Ag' \rangle \big) \,\mathrm{d}t \\
&= \int_0^{t_n} \langle \widetilde{e}'' + A\widetilde{e},\, g' \rangle \,\mathrm{d}t = -\int_0^{t_n} \langle \widetilde{R},\, g' \rangle \,\mathrm{d}t \\
&\le \max_{t \in [0,\, t_n]} |g'(t)| \int_0^{t_n} |\widetilde{R}| \,\mathrm{d}t \le |\widetilde{e}'(t_n)| \int_0^{t_n} |\widetilde{R}| \,\mathrm{d}t, \qquad (33)
\end{aligned}$$

where we have used (7), (8), (15) and (32). As a direct consequence of (33) we get

$$|\dot{e}_-^n| \le \int_0^{t_n} |\widetilde{R}| \,\mathrm{d}t.$$

To sum up, we have

Theorem 3.1. *Let u and U be the solutions of* (1) *and* (3)*, respectively. Then, for $1 \le n \le N$, there holds*

$$|u'(t_n) - \dot{U}_-^n| \le \int_0^{t_n} |\widetilde{R}| \,\mathrm{d}t, \tag{34}$$

where the a-posteriori quantity $\widetilde{R}$ is given by (14)*.*

Remark 3.2. Suppose that $u_0 \in D(A^2)$, $v_0 \in D(A^{3/2})$, and f lies in $L^2(0, T; D(A^{3/2}))$ and admits one time derivative. Then we have from (19) and Theorem 2.5 that the order of $\int_0^{t_n} |\widetilde{R}| \,\mathrm{d}t$ with respect to the time step is one. Hence, (34) gives us sharp a posteriori error estimates at the nodes.

4. An adaptive algorithm

Based on the a-posteriori error estimates given in Theorem 2.3, it is possible for us to construct an adaptive time stepping strategy related to the method (3). Let ϵ be the total error tolerance allowed for the a-posteriori error estimate in (23), i.e.,

$$\eta := \max_{1 \le m \le N} k_m |\widetilde{U}''|_{L^\infty(J_m)} + 2 \int_0^T |\widetilde{R}(s)| \,\mathrm{d}s \le \epsilon. \tag{35}$$

To ensure (35) holds, a natural way is to adjust the time step size k_m such that the following conditions are satisfied:

$$k_m |\widetilde{U}''|_{L^\infty(J_m)} \le \frac{1}{2}\epsilon, \qquad 2\frac{T}{k_m} \int_{t_{m-1}}^{t_m} |\widetilde{R}(s)| \,\mathrm{d}s \le \frac{1}{2}\epsilon,$$

which motivates us to use the following time-stepping strategy

$$\Theta := 2 \max \left\{ k_m |\widetilde{U}''|_{L^\infty(J_m)}, \quad 2\frac{T}{k_m} \int_{t_{m-1}}^{t_m} |\widetilde{R}(s)| \,\mathrm{d}s \right\} \le \epsilon. \tag{36}$$

TABLE 1. Example 1: order of Etd, Et and $\mathcal{E}_1$.

N	Etd	Order	Et	Order	$\mathcal{E}_1$	Order
16	5.5817e–1		3.7219e–1		1.7002	
32	2.7794e–1	1.0059	1.8787e–1	9.8631e–1	8.5476e–1	9.9213e–1
64	1.3859e–1	1.0040	9.4383e–2	9.9313e–1	4.2843e–1	9.9644e–1
128	6.9189e–2	1.0022	4.7308e–2	9.9644e–1	2.1444e–1	9.9853e–1
256	3.4565e–2	1.0012	2.3682e–2	9.9828e–1	1.0727e–1	9.9925e–1
512	1.7276e–2	1.0006	1.1849e–2	9.9907e–1	5.3650e–2	9.9963e–1
1024	8.6364e–3	1.0003	5.9264e–3	9.9951e–1	2.6829e–2	9.9982e–1
2048	4.3175e–3	1.0002	2.9635e–3	9.9984e–1	1.3415e–2	9.9991e–1
4096	2.1587e–3	1.0000	1.4819e–3	9.9984e–1	6.7078e–3	9.9995e–1

We mention that in the derivation of the above time stepping rule, the well known error equidistribution strategy are borrowed as used in [6,16]. Now, using (36) and following some ideas implied in the Runge-Kutta-Felberg method (cf. [21]), we can devise the following adaptive algorithm to control the time step size at each time step m.

Algorithm 4.1. *(Time step size control)*

(1) Given an error tolerance ϵ and a parameter $\delta \in (0, 1)$. Also assume that we have maximum and minimum for the time step size, denoted $k_{\max}$ and $k_{\min}$. These terms may be specified by the user, or they may be set to default values in a given software package.
(2) At the node t_{m-1}, begin with an initial step size, k_m.
(3) Compute $\dot{U}_-^m$ using (3) with the step size k_m. And then get U, U' and Θ at this time step.
(4) If $\delta\epsilon \le \Theta \le \epsilon$, then $U'(t)$ is an acceptable approximation of $u'(t)$, $t \in (t_{m-1}, t_{m-1}+k_m]$. The step size k_m is acceptable, and it is used to advance to the next grid point, $k_{m+1} = k_m$.
(5) If $\Theta < \delta\epsilon$, the step size is more than adequate, and we try to increase it. We double the step size as long as the larger step size is still smaller than $k_{\max}$. That is, we set $k_{m+1} = 2k_m$.
(6) If $\Theta > \epsilon$, then we decrease the step size. Replace $k_m = \frac{1}{2}k_m$ provided that the smaller step size satisfies $k_m \ge k_{\min}$. Return to Step (3), where new values of $\dot{U}_-^m$ and U, U', Θ are computed for this smaller step size.

Remark 4.2. If the time step k_m ($m = 1, 2, \ldots$) determined by the above algorithm all lie in $(k_{\min}, k_{\max})$, then we easily have from (23), (36) and the definition of η (cf. (35)) that

$$|(u - U)'|_{L^\infty(0,\,T)} \le \eta \le \epsilon.$$

5. Numerical Experiments

5.1. Efficiency of the estimators. In this subsection, we want to demonstrate the performance of the a-posteriori error estimators in Sections 2 and 3, in terms of some efficiency indices.

TABLE 2. Example 1: order of Ed and $\mathcal{E}_1 + \mathcal{E}_2$.

N	Ed	Order	$\mathcal{E}_1 + \mathcal{E}_2$	Order
16	1.0609		3.2251	
32	5.4718e–1	9.5523e–1	1.6554	9.6215e–1
64	2.7770e–1	9.7846e–1	8.3851e–1	9.8131e–1
128	1.3987e–1	9.8945e–1	4.2193e–1	9.9083e–1
256	7.0189e–2	9.9478e–1	2.1164e–1	9.9541e–1
512	3.5158e–2	9.9740e–1	1.0599e–1	9.9771e–1
1024	1.7595e–2	9.9871e–1	5.3035e–2	9.9886e–1
2048	8.8012e–3	9.9935e–1	2.6528e–2	9.9943e–1
4096	4.4016e–3	9.9968e–1	1.3267e–2	9.9971e–1

TABLE 3. Example 1: order of $\mathcal{E}_2$ and $\mathcal{E}_3$.

N	$\mathcal{E}_2$	Order	Ed	Ed+Etd	$\mathcal{E}_3$	Order
16	1.5249		1.0609	1.6191	4.9253	
32	8.0067e–1	9.2943e–1	5.4718e–1	8.2512e–1	2.5102	9.7243e–1
64	4.1008e–1	9.6532e–1	2.7770e–1	4.1629e–1	1.2669	9.8645e–1
128	2.0749e–1	9.8282e–1	1.3987e–1	2.0906e–1	6.3636e–1	9.9343e–1
256	1.0436e–1	9.9145e–1	7.0189e–2	1.0475e–1	3.1891e–1	9.9670e–1
512	5.2336e–2	9.9574e–1	3.5158e–2	5.2433e–2	1.5964e–1	9.9835e–1
1024	2.6207e–2	9.9787e–1	1.7595e–2	2.6231e–2	7.9864e–2	9.9918e–1
2048	1.3113e–2	9.9894e–1	8.8012e–3	1.3119e–2	3.9943e–2	9.9959e–1
4096	6.5590e–3	9.9947e–1	4.4016e–3	6.5603e–3	1.9975e–2	9.9980e–1

Example 1. As in [1], we consider an ordinary differential equation given by

$$\begin{cases} u''(t) + 2u(t) = 2e^t(\cos t - \sin t), \quad 0 < t < 2, \\ u(0) = 1, \\ u'(0) = 1, \end{cases}$$

which has the exact solution $u(t) = e^t \cos t$ and $\|\cdot\| = \sqrt{2}|\cdot|$.

In our numerical computation, we make a uniform partition for the domain $[0, 2]$, so that $k_m = 2/N$, $1 \le m \le N$. Here N is a given natural number. For simplicity, write

$$\mathcal{E}_1 := 2\int_0^2 |\widetilde{R}(s)|\,\mathrm{d}s, \qquad \mathcal{E}_2 := \max_{1\le m\le N} k_m |\widetilde{U}''|_{L^\infty(J_m)}, \quad \mathcal{E}_3 := 2\mathcal{E}_1 + \mathcal{E}_2,$$

$$\mathrm{Ed} := \big|(u-U)'\big|_{L^\infty(0,\,2)}, \qquad \mathrm{Et} := \max_{0\le\tau\le 2} \|(u-\widetilde{U})(\tau)\|,$$

$$\mathrm{Etd} := \max_{0\le\tau\le 2} |(u-\widetilde{U})'(\tau)|, \quad \mathrm{Esd} := |u'(2) - \dot{U}_-^N|.$$

In Tables 1-4 we give the values of a posteriori error estimators $\mathcal{E}_1$, $\mathcal{E}_2$ and $\mathcal{E}_3$ as well as their orders. These numerical results confirm the theoretical results of Theorems 2.1, 2.3, Corollary 2.4 and Theorem 3.1, respectively.

Next, we study the efficiency of the lower and upper estimators in Corollary 2.4, using the indices as given in [1]. With respect to the reference error Ed+Etd the lower effectivity index Effld and the upper effectivity index Effud are defined as

$$\mathrm{Effld} := \frac{\mathcal{E}_2}{\mathrm{Ed{+}Etd}}, \quad \mathrm{Effud} := \frac{\mathcal{E}_3}{\mathrm{Ed{+}Etd}},$$

TABLE 4. Example 1: order of Esd.

N	Esd	Order	$\mathcal{E}_1/2$	Order
16	5.5824e–1		8.5011e–1	
32	2.7797e–1	1.0060	4.2738e–1	9.9213e–1
64	1.3861e–1	1.0039	2.1422e–1	9.9644e–1
128	6.9196e–2	1.0022	1.0722e–1	9.9853e–1
256	3.4570e–2	1.0012	5.3637e–2	9.9925e–1
512	1.7278e–2	1.0006	2.6825e–2	9.9963e–1
1024	8.6370e–3	1.0003	1.3414e–2	9.9982e–1
2048	4.3181e–3	1.0002	6.7076e–3	9.9991e–1
4096	2.1589e–3	1.0001	3.3539e–3	9.9995e–1

TABLE 5. Example 1: effectivity indices of lower and upper estimators.

N	Effld	Effud
16	9.4183e–1	3.0420
32	9.7037e–1	3.0422
64	9.8507e–1	3.0434
128	9.9251e–1	3.0439
256	9.9628e–1	3.0444
512	9.9815e–1	3.0446
1024	9.9908e–1	3.0447
2048	9.9957e–1	3.0448
4096	9.9979e–1	3.0447

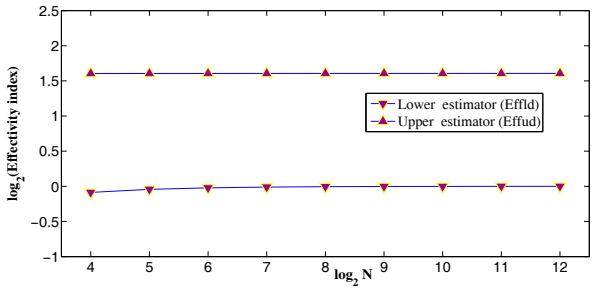

FIGURE 1. Log-log graphs of the effectivity indices of lower and upper estimators (the base of the logarithms is 2).

respectively. We compute these indices in Table 5 and graphically demonstrate them in log-log scale in Figure 1. It is observed that Effld≈ 1, Effud≈ 3.

5.2. Efficiency of the adaptive algorithm.

Example 2. In order to test the effectiveness of our adaptive algorithm (Algorithm 4.1), we first consider the ODE case (cf. (1)) with $A = 2$, $T = 10$, and the right term f is taken such that the exact solution of (1) is

$$u(t) = \alpha(t) := e^{-800(\sin(\pi t/2)-1)^2} \sin(4\pi t). \tag{37}$$

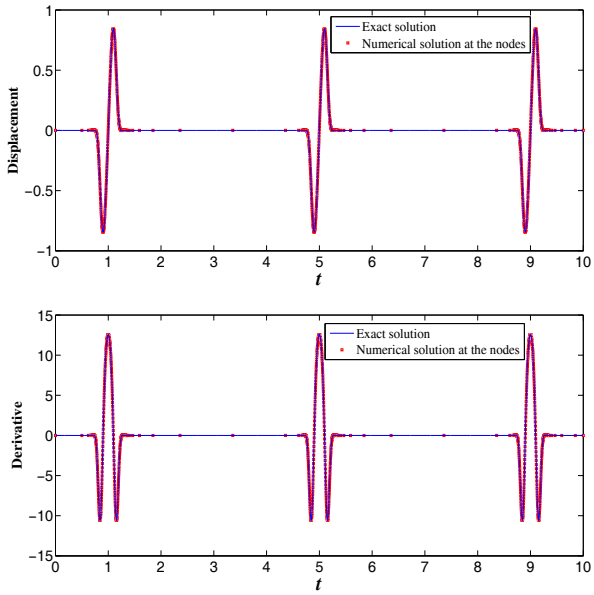

FIGURE 2. Example 2: solution curve (top) and derivative curve (bottom) with $\epsilon = 1$, $k_{\min} = 2 * 10^{-3}$.

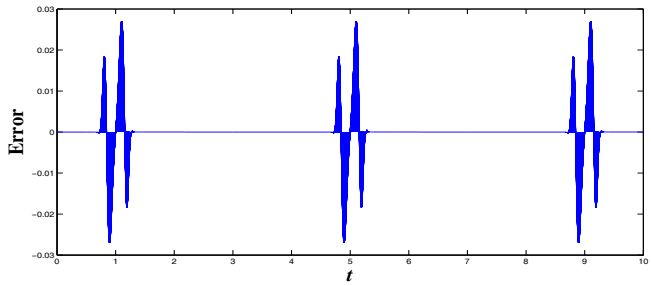

(a)

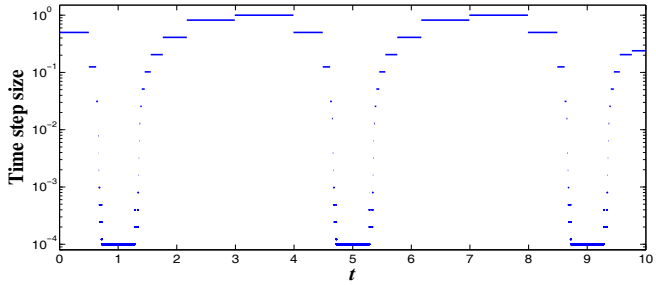

(b)

FIGURE 3. Example 2: (a) the error of $(u - U)'(t)$ and (b) the time stepsize trajectory, with $\epsilon = 10^{-1}$, $k_{\min} = 10^{-4}$.

TABLE 6. Example 2: adaptive numerical results with different ϵ and $k_{\min}$.

ϵ	$k_{\min}$	η	$\lvert(u-U)'\rvert_{L^\infty(0,\,T)}$	N	N_*
1	2e–3	5.9936	5.4037e–1	1013	1045
1	1e–3	3.0014	2.7031e–1	1860	1895
1	2e–4	6.1008e–1	5.4086e–2	8553	8600
1e–1	1e–4	3.0162e–1	2.7033e–2	18175	18231
1e–1	5e–5	1.5140e–1	1.3518e–2	34994	35052
1e–1	3e–5	9.1402e–2	8.1124e–3	57183	57243
1e–2	1e–5	3.0189e–2	2.7035e–3	180730	180806
1e–2	3e–6	9.1552e–3	8.1131e–4	570458	570538

TABLE 7. Example 2: numerical results with uniform partitions.

N_*	η	$\lvert(u-U)'\rvert_{L^\infty(0,\,T)}$
1045	2.8677e+1	2.5809
1895	1.5813e+1	1.4261
8600	3.4823	3.1436e–1
18231	1.6443	1.4830e–1
35052	8.5795e–1	7.7130e–2
57243	5.2535e–1	4.7229e–2
180806	1.6632e–1	1.4953e–2
570538	5.2708e–2	4.7385e–3

TABLE 8. Example 3: adaptive numerical results with different ϵ and $k_{\min}$, $k_{\max} = 1$, Case (A).

ϵ	$k_{\min}$	η	$\lvert(u-U)'\rvert_{L^\infty(0,\,T)}$	N	N_*
1	1e–3	2.0652	1.9882e–1	1830	1864
1	2e–4	4.2311e–1	4.0006e–2	8483	8530
1e–1	1e–4	2.0740e–1	1.9867e–2	17724	17779
1e–1	5e–5	1.0422e–1	9.9400e–3	34474	34531
1e–2	1e–5	2.1623e–2	1.9925e–3	176333	176401
1e–2	4e–6	8.4844e–3	8.0505e–4	428114	428188

We set $k_{\max} = 1$ and $\delta = 1/32$ in the computation. In Figure 2 we give the numerical solutions for u and u'. The error of $(u-U)'(t)$ is depicted in Figure 3(a) and the time stepsize trajectory is shown in Figure 3(b). In Table 6 we have reported the numerical results when running the adaptive algorithm for different values of ϵ and $k_{\min}$, where (N_*-1) is the total number of the time iterative step in the adaptive computation. Moreover, we adopt the uniform partitions to compute with the same iteration number (N_*-1), and the numerical results are shown in Table 7, from which we know the adaptive algorithm is very efficient.

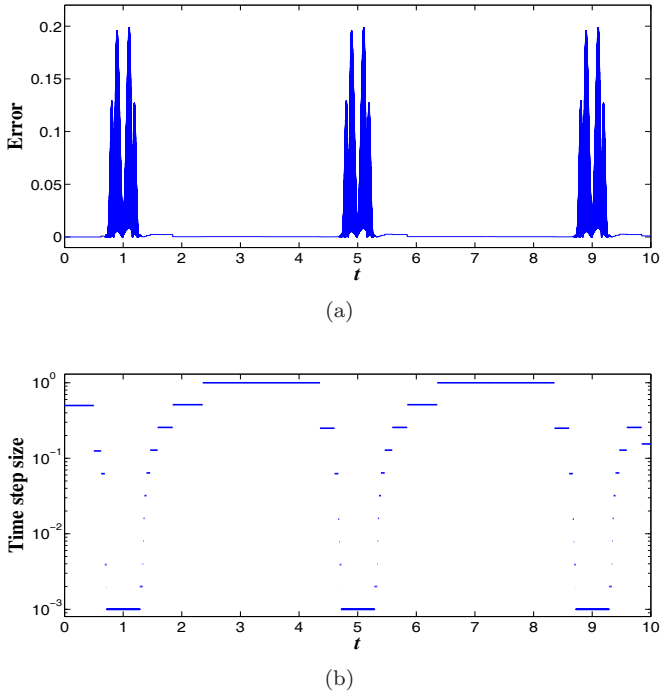

(a)

(b)

FIGURE 4. Example 3: (a) the error of $|(u-U)'(t)|$ and (b) the time stepsize trajectory, with $\epsilon = 1$, $k_{\min} = 10^{-3}$, $k_{\max} = 1$, case (A).

Example 3. Next, we discuss numerical results in the 1-dim PDE case. The problem under investigation is

$$\text{(38)} \qquad \begin{cases} \dfrac{\partial^2 u}{\partial t^2} - 2\dfrac{\partial^2 u}{\partial x^2} = f(x,\,t), & 0 < x < 1,\ 0 < t < T, \\ u(0,\,t) = u(1,\,t) = 0, & 0 < t \le T, \\ u(x,\,0) = u_0(x), \quad \dfrac{\partial u}{\partial t}(x,\,0) = v_0(x), & 0 \le x \le 1. \end{cases}$$

Choose the solution of (38) by

$$\begin{aligned} &\text{Case (A)} \qquad u(x,\,t) = \alpha(t) * \sin(\pi x), \quad T = 10, \\ &\text{Case (B)} \qquad u(x,\,t) = \beta(t) * \sin(\pi x), \quad T = 1, \end{aligned}$$

where $\alpha(t)$ is given in (37) and $\beta(t) = 0.1 * (1 - e^{-10000*(t-1/2)^2})$, which is used in [6] for numerical experiments.

We apply Algorithm 4.1 to solve these problems. We choose $\delta = 1/32$ in computation. For the spatial discretization, we use linear finite element on a uniform partition with the mesh size equal to 1/20000. The error of $|(u-U)'(t)|$ and the time step size at each time step are displayed in Figures 4-5. The adaptive numerical results with different ϵ and $k_{\min}$ are shown in Tables 8-9, and the numerical results with uniform partitions are shown in Tables 10-11, from which we may find that Algorithm 4.1 is also very efficient in this PDE case.

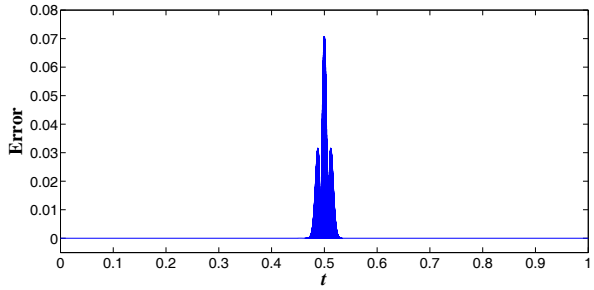

(a)

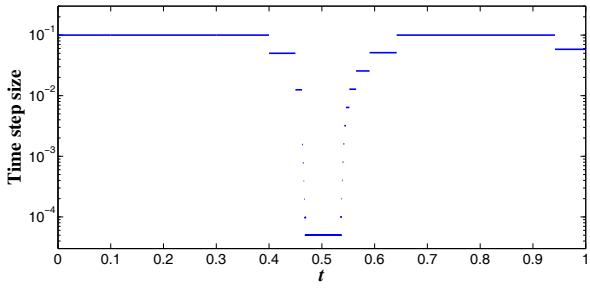

(b)

FIGURE 5. Same as Figure 4, except for Case (B) with $\epsilon = 10^{-1}$, $k_{\min} = 5 * 10^{-5}$, $k_{\max} = 10^{-1}$.

TABLE 9. Example 3: adaptive numerical results with different ϵ and $k_{\min}$, $k_{\max} = 10^{-1}$, Case (B).

ϵ	$k_{\min}$	η	$\lvert(u-U)'\rvert_{L^\infty(0,T)}$	N	N_*
1e–1	1e–4	4.0947e–1	1.4149e–1	732	743
1e–1	5e–5	2.0522e–1	7.0745e–2	1399	1411
1e–1	1e–5	4.1451e–2	1.4150e–2	6323	6338
1e–2	1e–5	4.1056e–2	1.4149e–2	7144	7160
1e–2	5e–6	2.0549e–2	7.0746e–3	13804	13821
1e–2	2e–6	8.2486e–3	2.8299e–3	32855	32873
1e–3	2e–6	8.2086e–3	2.8298e–3	36743	36760
1e–3	2e–7	8.2608e–4	2.8299e–4	328825	328845

Example 4. Now, let us discuss the cantilever beam case. The problem under investigation is

$$
\begin{cases}
\dfrac{\partial^2 u}{\partial t^2} + \dfrac{\partial^4 u}{\partial x^4} = f(x,t), & 0 < x < 1,\ 0 < t < T,\\
u(0,t) = 0, \quad \dfrac{\partial u}{\partial x}(0,t) = 0, & 0 < t \le T,\\
\dfrac{\partial^2 u}{\partial x^2}(1,t) = 0, \quad \dfrac{\partial^3 u}{\partial x^3}(1,t) = 0, & 0 < t \le T,\\
u(x,0) = u_0(x), \quad \dfrac{\partial u}{\partial t}(x,0) = v_0(x), & 0 \le x \le 1.
\end{cases} \tag{39}
$$

TABLE 10. Example 3: numerical results with uniform partitions, Case (A).

N_*	η	$\|(u-U)'\|_{L^\infty(0,T)}$
1864	1.1046e+1	1.0750
8530	2.4126	2.3534e–1
17779	1.1584	1.1292e–1
34531	5.9831e–1	5.8142e–2
176401	1.1711e–1	1.1382e–2
428188	4.8245e–2	4.6890e–3

TABLE 11. Example 3: numerical results with uniform partitions, Case (B).

N_*	η	$\|(u-U)'\|_{L^\infty(0,T)}$
743	5.4930	1.8726
1411	2.8976	9.9845e–1
6338	6.4555e–1	2.2326e–1
7160	5.7145e–1	1.9763e–1
13821	2.9625e–1	1.0238e–1
32873	1.2480e–1	4.3043e–2
36760	1.1160e–1	3.8491e–2
328845	1.2475e–2	4.3027e–3

TABLE 12. Example 4: adaptive numerical results with different ϵ and $k_{\min}$, $k_{\max} = 10^{-1}$.

ϵ	$k_{\min}$	η	$\|(u-U)'\|_{L^\infty(0,T)}$	N	N_*
1e–1	1e–4	7.26e–2	2.47e–2	668	693
1e–1	5e–5	3.65e–2	1.24e–2	1267	1294
1e–2	1e–5	7.29e–3	2.47e–3	6540	6571
1e–2	5e–6	3.69e–3	1.24e–3	12556	12589

Choose the exact solution of (39) by

$$u(x,t) = \beta(t) * 0.01(x^6 - 20x^3 + 45x^2), \quad T = 1,$$

where $\beta(t)$ is given as in Example 3.

We apply Algorithm 4.1 with $\delta = 1/32$ to solve this problems. We carry out the spatial discretization using Hermitian beam element on a uniform partition with the mesh size equal to 1/200. The error of $|(u-U)'(t)|$ and the time step size at each time step are displayed in Figure 6. The adaptive numerical results with different ϵ and $k_{\min}$ are shown in Table 12, and the numerical results with uniform partitions are shown in Table 13, from which we may find that Algorithm 4.1 is also efficient in this cantilever beam case.

Example 5. In this example, we discuss the 2-dim PDE case. The problem is governed by

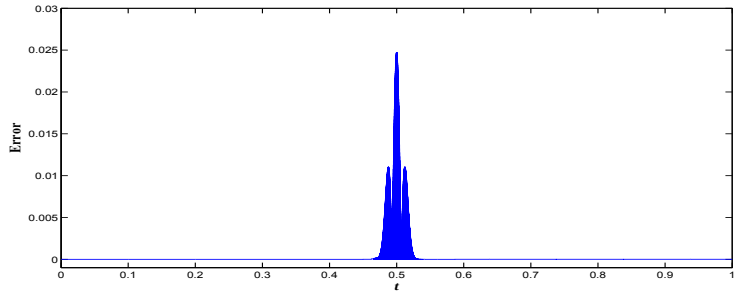

(a)

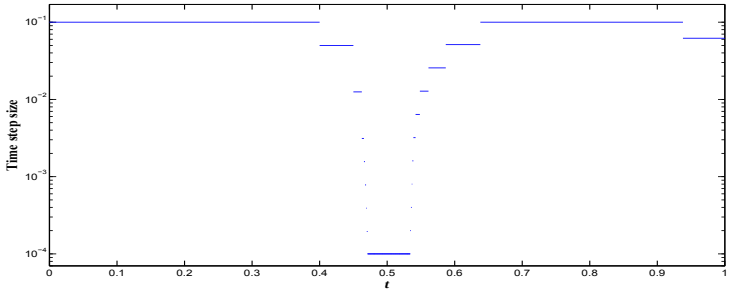

(b)

FIGURE 6. Example 4: (a) the error of $|(u-U)'(t)|$ and (b) the time stepsize trajectory, with $\epsilon = 10^{-1}$, $k_{\min} = 10^{-4}$, $k_{\max} = 10^{-1}$.

TABLE 13. Example 4: numerical results with uniform partitions.

N_*	η	$\lvert(u-U)'\rvert_{L^\infty(0,T)}$
693	1.05	3.55e–1
1294	5.62e–1	1.90e–1
6571	1.10e–1	3.76e–2
12589	5.75e–2	1.96e–2

$$
(40)\qquad \begin{cases} \dfrac{\partial^2}{\partial t^2}u(x,y,t) - \Delta u(x,y,t) = f(x,y,t) & \text{in } \Omega\times(0,T), \\ u(x,y,t) = u_b(x,y,t) & \text{on } \partial\Omega\times(0,T], \\ u(x,y,0) = u_0(x,y) & \text{on } \Omega\times\{0\}, \\ \dfrac{\partial}{\partial t}u(x,y,0) = v_0(x,y) & \text{on } \Omega\times\{0\}. \end{cases}
$$

We set $\Omega = (-3/2, 3/2)\times(-3/2, 3/2)$ and $T = 1$. The exact solution of this problem is prescribed as

$$u(x,y,t) = \beta(t) * e^{-((x-t+0.5)^2+(y-t+0.5)^2)/0.04},$$

where $\beta(t)$ is given as in Example 3.

We use the continuous P_1-element to carry out spatial discretization. And then apply Algorithm 4.1 ($\delta = 1/8$) to compute the discrete problem in time. Notice

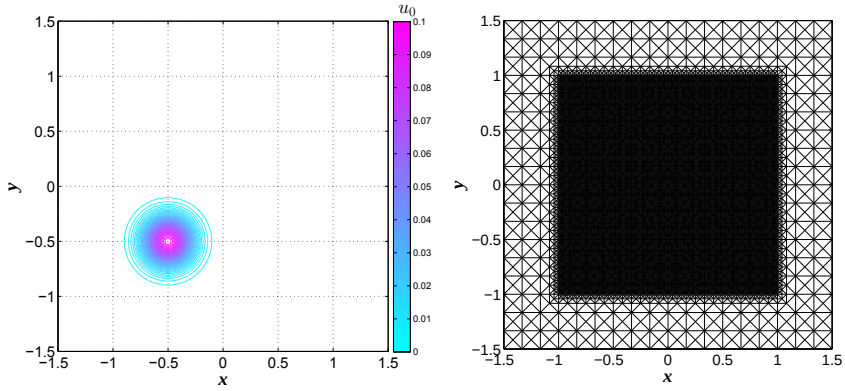

(a) Initial function (b) Mesh

FIGURE 7. Example 5: initial function u_0 & mesh.

TABLE 14. Example 5: adaptive numerical results with different ϵ, $k_{\min}$, and $k_{\max}$.

ϵ	$k_{\max}$	$k_{\min}$	η	$\lvert(u-U)'\rvert_{L^\infty(0,T)}$	N	N_*
5	1e–2	1e–3	1.76	4.71e–1	156	165
5	1e–2	1e–4	5.11e–1	4.97e–2	566	581
1	1e–3	5e–5	1.10e–1	2.33e–2	1989	2000
0.5	5e–4	1e–5	3.52e–2	5.14e–3	6162	6177

TABLE 15. Example 5: numerical results with uniform partitions.

N_*	η	$\lvert(u-U)'\rvert_{L^\infty(0,T)}$
165	8.14	2.66
581	2.50	8.16e–1
2000	7.24e–1	2.38e–1
6177	2.34e–1	7.70e–2

that the graph of the function $u = u(x, y, t)$ looks like a "Hill" moving from point $(-1/2, -1/2)$ straightly to point $(1/2, 1/2)$ and drops exponentially around $t = 0.5$. To reduce the computational cost, thinking of the decay property of the exact function, we make a coarse partition in the whole spatial domain with the mesh size equal to $1/6$, and then do the mesh refinement in the domain $(-1, 1) \times (-1, 1)$ to get a refined mesh with the size equal to $1/48$, as shown in Figure 7.

The error of $|(u-U)'(t)|$ and the time step size are displayed in Figure 8, and the numerical solution with $\epsilon = 1$, $k_{\min} = 5 * 10^{-5}$, $k_{\max} = 10^{-3}$ at different time are shown in Figure 9. The adaptive numerical results with different ϵ ,$k_{\min}$ and $k_{\max}$ are shown in Table 14, and the numerical results with uniform partitions in time step are shown in Table 15, from which we may see the effectiveness of Algorithm 4.1 in this 2-dim PDE case.

In the last part of this section, we summarize some key observations from the above numerical results:

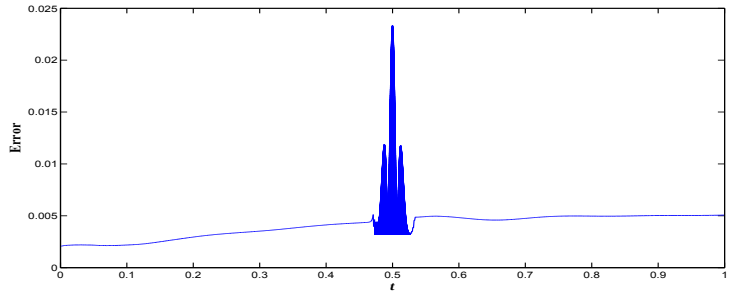

(a)

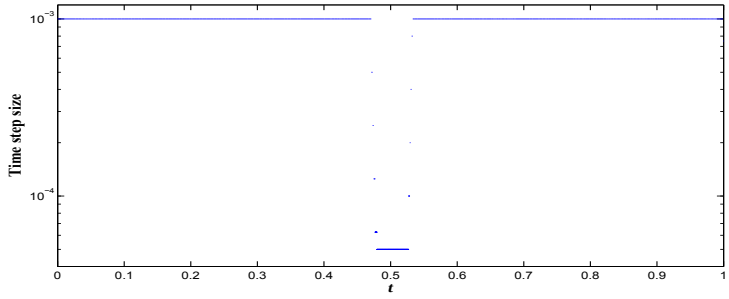

(b)

FIGURE 8. Example 5: (a) the error of $|(u-U)'(t)|$ and (b) the time stepsize trajectory, with $\epsilon = 1$, $k_{\min} = 5 * 10^{-5}$, $k_{\max} = 10^{-3}$.

- The a-posteriori error estimators given in Section 2 are reliable and efficient. Algorithm 4.1 is efficient for solving evolution problems under discussion. This can be demonstrated by comparing the numerical errors obtained through the uniform partition and adaptive partition, see, e.g. Tables 7 and 6, Tables 10 and 8, Tables 11 and 9, Tables 13 and 12, Tables 15 and 14.
- The choice of $k_{\min}$ is essential in keeping high efficiency of Algorithm 4.1. If it is chosen too large, the total error may exceed the prescribed error tolerance; and if too small, the algorithm may result in over-refinement. In practical computation, this parameter can be chosen quite easily by numerical experience. However, it is a very valuable issue to develop some rules for feasibly choosing $k_{\min}$ with theoretical justification.

Acknowledgments

The authors would like to thank the three anonymous referees for their valuable and insightful comments which greatly improved the early version of the paper. They also thank the Ph.D. candidate Huashan Sheng of the second author for his critical support in conducting numerical experiments for Examples 4 and 5 in the last section of this paper.

References

[1] G. Akrivis and P. Chatzipantelidis, A posteriori error estimates for the two-step backward differentiation formula method for parabolic equations, SIAM J. Numer. Anal., 48 (2010) 109–132.

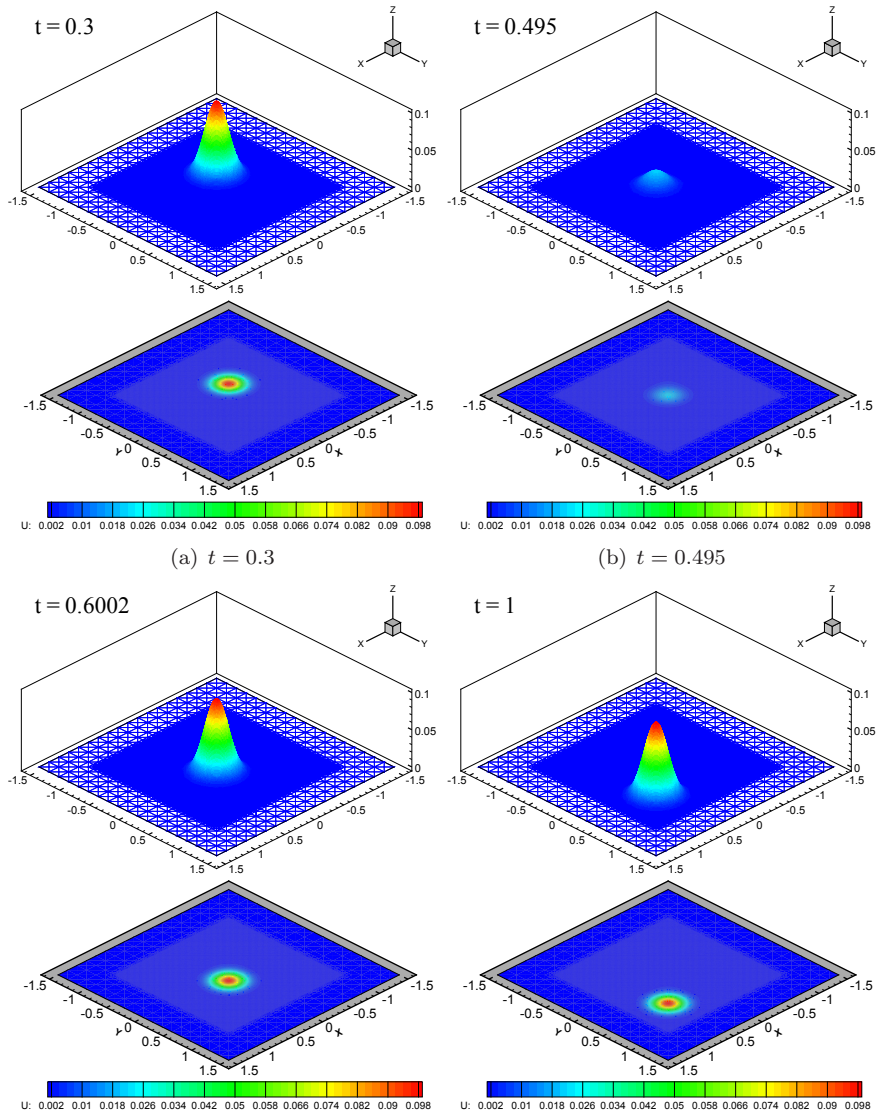

(a) $t = 0.3$ (b) $t = 0.495$

(c) $t = 0.6002$ (d) $t = 1$

FIGURE 9. Example 5: surface and contour plots of numerical solutions at time t = 0.3; 0.495; 0.6002; 1, with $\epsilon = 1$, $k_{\min} = 5 * 10^{-5}$, $k_{\max} = 10^{-3}$.

[2] G. Akrivis, C. Makridakis and R.H. Nochetto, A posteriori error estimates for the Crank-Nicolson method for parabolic equations, Math. Comp., 75 (2006) 511–531.
[3] G. Akrivis, C. Makridakis and R.H. Nochetto, Optimal order a posteriori error estimates for a class of Runge-Kutta and Galerkin methods, Numer. Math., 114 (2009) 133–160.
[4] G. Akrivis, C. Makridakis and R.H. Nochetto, Galerkin and Runge-Kutta methods: unified formulation, a posteriori error estimates and nodal superconvergence, Numer. Math., 118 (2011) 429–456.
[5] C. Bernardi and E. Süli, Time and space adaptivity for the second-order wave equation, Math. Models Methods Appl. Sci., 15 (2005) 199–225.

[6] Z. Chen and J. Feng, An adaptive finite element algorithm with reliable and efficient error control for linear parabolic problems, Math. Comp., 73 (2004) 1167–1193.
[7] E. Georgoulis, O. Lakkis and C. Makridakis, A posteriori $L^\infty(L^2)$-error bounds for finite element approximations to the wave equation, IMA J. Numer. Anal., 33 (2013) 1245–1264.
[8] J. Huang, J. Lai and T. Tang, An adaptive time stepping method with efficient error control for second-order evolution problems, Sci. China Math., 56 (2013) 2753–2771.
[9] T.J.R. Hughes, The Finite Element Method: Linear Static and Dynamic Finite Element Analysis, Dover Publications, New York, 2000.
[10] D. Kessler, R.H. Nochetto and A. Schmidt, A posteriori error control for the Allen–Cahn problem: circumventing Gronwall's inequality, ESAIM-Math. Model. Num., 38 (2004) 129–142.
[11] J. Lai, J. Huang and C. Chen, Vibration analysis of plane elasticity problems by the C^0-continuous time stepping finite element method, Appl. Numer. Math., 59 (2009) 905–919.
[12] J. Lai, J. Huang and Z. Shi, Vibration analysis for elastic multi-beam structures by the C^0-continuous time-stepping finite element method, Int. J. Numer. Meth. Biomed. Engng., 26 (2010) 205–233.
[13] J. Lai, Q. Wang and J. Huang, C^0-continuous time stepping linear finite element method for second order linear hyperbolic equations (in Chinese), J. Shanghai Jiaotong Univ., 42 (2008) 2065–2069.
[14] C. Makridakis and R.H. Nochetto, A posteriori error analysis for higher order dissipative methods for evolution problems, Numer. Math., 104 (2006) 489–514.
[15] S.E. Minkoff and N.M. Kridler, A comparison of adaptive time stepping methods for coupled flow and deformation modeling, Appl. Math. Model., 30 (2006) 993–1009.
[16] R.H. Nochetto, G. Savaré and C. Verdi, A posteriori error estimates for variable time-step discretizations of nonlinear evolution equations, Comm. Pure. Appl. Math., 53 (2000) 525–589.
[17] Z. Qiao, Z. Zhang and T. Tang, An adaptive time-stepping strategy for the molecular beam epitaxy models, SIAM J. Sci. Comput., 33 (2011) 1395–1414.
[18] A. Quarteroni, R. Sacco and F. Saleri, Numerical Mathematics, Springer, Berlin, 2000.
[19] M. Renardy and R.C. Rogers, An Introduction to Partial Differential Equations, 2nd ed., Springer, Berlin, 2004.
[20] J. Shen, T. Tang and L. Wang, Spectral Methods: Algorithms, Analysis and Applications, Springer, Berlin, 2011.
[21] J. Stoer and R. Bulirsch, Introduction to Numerical Analysis, 3rd ed., Springer, New York, 2002.
[22] Z. Tan, Z. Zhang, Y. Huang and T. Tang, Moving mesh methods with locally varying time steps, J. Comput. Phys., 200 (2004) 347–367.
[23] V. Thomée, Galerkin Finite Element Methods for Parabolic Problems, 2nd ed., Springer, Berlin, 2006.
[24] R. Verfürth, A Review of A Posteriori Estimation and Adaptive Mesh–Refinement Techniques, Wiley-Teubner, Chichester, 1996.
[25] J. Wloka, Partial Differential Equations, Cambridge University Press, Cambridge, 1987.
[26] C. Xu and T. Tang, Stability analysis of large time-stepping methods for epitaxial growth models, SIAM J. Numer. Anal., 44 (2006) 1759–1779.
[27] Z. Zhang and Z. Qiao, An adaptive time-stepping strategy for the Cahn-Hilliard equation, Commun. Comput. Phys., 11 (2012) 1261–1278.

Department of Mathematics, Minjiang University, Fuzhou 350108, China
E-mail: laijunjiang@sjtu.org

Department of Mathematics, and MOE-LSC, Shanghai Jiao Tong University, Shanghai 200240, China, and Division of Computational Science, E-Institute of Shanghai Universities, Shanghai Normal University, China
E-mail: jghuang@sjtu.edu.cn